Biochemical and Biophysical Research Communications 451 (2014) 15–23

Contents lists available at ScienceDirect

Biochemical and Biophysical Research Communications

journal homepage: www.elsevier.com/locate/ybbrc

Protecting capacity against malaria of chemically defined tetramer forms based on the *Plasmodium falciparum* apical sushi protein as potential vaccine components

Magnolia Vanegas [a,b], Adriana Bermúdez [a], Yuly Andrea Guerrero [a], Jesús Alfredo Cortes-Vecino [b], Hernando Curtidor [a], Manuel Elkin Patarroyo [a,b], José Manuel Lozano [a,b,*]

[a] *Fundación Instituto de Inmunología de Colombia (FIDIC) – Universidad del Rosario, Bogotá, Colombia*
[b] *Universidad Nacional de Colombia, Bogotá, Colombia*

ARTICLE INFO

Article history:
Received 24 June 2014
Available online 22 July 2014

Keywords:
Plasmodium
*Pf*ASP
Dendrimer
Macromolecule
Antimalarial-vaccine

ABSTRACT

Developing novel generations of subunit-based antimalarial vaccines in the form of chemically-defined macromolecule systems for multiple antigen presentation represents a classical problem in the field of vaccine development. Many efforts involving synthesis strategies leading to macromolecule constructs have been based on dendrimer-like systems, the condensation of large building blocks and conventional asymmetric double dimer constructs, all based on lysine cores.

This work describes novel symmetric double dimer and condensed linear constructs for presenting selected peptide multi-copies from the apical sushi protein expressed in *Plasmodium falciparum*. These molecules have been proved to be safe and innocuous, highly antigenic and have shown strong protective efficacy in rodents challenged with two *Plasmodium* species. Insights into systematic design, synthesis and characterisation have led to such novel antigen systems being used as potential platforms for developing new anti-malarial vaccine candidates.

1. Introduction

Malaria continues to be a worldwide public health problem, severely affecting the poorest communities' health and economic welfare. The World Health Organization (WHO) estimated in its 2012 annual report that around 216 million clinical episodes occur and about 655,000 deaths are caused annually, mainly by *Plasmodium falciparum* [1]. It has been estimated that the economic and social burden caused by malaria is high; the worsening situation highlights the lack of effective vaccines [2]. Nearly 150 antimalarial vaccine prototype candidates are currently being evaluated; however, the results have been no better than those achieved 20 years ago with the first synthetic vaccine against this disease, the so-called SPf-66 [3].

Our institute has established a methodology enabling conserved parasite protein-derived antigen regions to identify peptide-motifs specifically binding to target liver and red blood cells (RBC). Critical-binding residues' systematic modification has led to obtaining new malarial peptide analogues which have induced a protective effect against *P. falciparum* [4,5].

However, the development of a chemically-defined antimalarial vaccine currently lacks a suitable platform system for multiple antigen presentation, in spite of the great success of SPf66 which was conceived as a macromolecule delivered via non-controlled cysteine polymers. The present work was thus aimed at obtaining large novel tetramer constructs for multi-copy antigen presentation; our design was thus based on the *Plasmodium* apical sushi protein (*Pf*ASP) as being a newly-described antigen expressed during parasite blood stages. The first step was to identify *Pf*ASP regions implicated in pathogen binding to its target cells as well as predicted HLA-DR reading frames; these conserved regions contain short peptides known as high activity binding peptides (HABPs). This was followed by strategic amino acid replacement, according to previous work [4], and then synthesis for modified HABPs. Two families of tetramer constructs were obtained by strategically spacing them as tetramer-branched forms from a novel symmetric lysine-based core, using cathepsin specific substrate sequences or aminohexanoic acid: equally spaced symmetric double dimer constructs (SDDCs) and condensed linear constructs (CLCs).

* Corresponding author at: Biocatalysis Department, Fundación Instituto de Inmunología de Colombia (FIDIC), Carrera 50 No. 26-20, ZIP 111321 Bogotá DC, Colombia. Fax: +57 1 481 5269.
E-mail addresses: jm_lozano@fidic.org.co, jmlozanom@unal.edu.co (J.M. Lozano).

http://dx.doi.org/10.1016/j.bbrc.2014.06.143
0006-291X/

2. Materials and methods

2.1. Predicting PfASP B-epitopes

The Antheprot and BepiPred servers were chosen for visualising and selecting four B-linear peptides for obtaining *Pf*ASP polyclonal antibodies [6].

The selected predicted peptide-epitopes were then synthesised by *t*-Boc solid-phase strategy. Putative B-epitopes were obtained as polymer forms by non-controlled polymerisation via cysteine-end residues; they were co-formulated with a non-specific T-epitope [7] and then used for immunising New Zealand rabbits.

2.2. Synthesis of PfASP, peptide ^{125}I-radiolabelling and detecting high activity human red blood cell binding peptides

The 731 amino acid-long *Pf*ASP was synthesised in its entirety as 20-mer non-overlapping peptides, the *t*-Boc synthesis strategy providing 37 peptides. A Tyr residue was added at the carboxyl end for ^{125}I-labelling peptides which did not contain this amino acid in their sequences [8,9].

2.3. PfASP peptides' in vitro inhibition of malarial invasion

*Pf*ASP native HABPs and their scrambled versions were tested for their ability to inhibit *P. falciparum* (FCB-2 strain) invasion of human RBCs in *in vitro* assays [10]. Parasitaemia was quantified by flow cytometry using FCAScan equipment (Becton Dickinson, San José, CA). Cell Quest software was used for recording and analysing experimental data. Invasion inhibition was calculated as being 100 × (% parasitaemia in control − % parasitaemia in test)/(% parasitaemia in control).

2.4. Immunochemical assays

Classical immunochemistry methodologies were used for assaying anti-*Pf*ASP antibody reactivity. Specific anti-test compound activity was detected using a dilution of either anti-mouse or anti-rabbit IgG-peroxidase-conjugate for enzyme-linked immunosorbent assay (ELISA) and Western blot (WB) tests. Anti-mouse and rabbit IgG-FITC conjugates (fluorescein isothiocyanate, Vector Laboratories, Inc. Burlingame, CA, USA) were used for indirect fluorescent antibody (IFA) tests which involved analysing antibody sera reactivity against *Plasmodiuṁs* blood-stage expressed proteins in infected RBC on glass slides. WB assays were performed on electrophoretically resolved *P. falciparum* protein schizont lysates transferred to nitrocellulose [9].

2.5. Macromolecule design, synthesis and physicochemical characterisation

2.5.1. Symmetric double dimer construct (SDDC)

The peptide synthesis methodology was modified for providing macromolecule constructs for coupling the third residue to build what we have called an SDDC. Two SDDCs were synthesised and coded 38987 and 38991. The difference consisted of the third residue (a *Fmoc*-Lys(ivDde)-OH) where ivDde is 1-(4,4-dimethyl-2,6-dioxocyclohex-1-ylidene)isovaleryl belonging to the macromolecule core allowing selective deprotection of the *Fmoc*-α-amino group to enable *Fmoc*-β-Ala-OH coupling. Lysine's *N*-ε function (ivDde) was deprotected with 2% hydrazine in DMF for 30 min and *Fmoc* groups were then deprotected. Molecular design proposed a β-Ala-Lys symmetric modelled platform in which distances between α-carbon to amino functions were 6.243 Å and 6.266 Å, respectively (ChemDraw Ultra 7.0-PerkinElmer); data were revised by using Accelrys Inc. software package 2000 (San Diego, CA, USA). β-Ala was also included in this macromolecule design, due to its proven capacity for stabilising secondary structure elements [11].

2.5.2. Condensed linear constructs (CLC)

CLC synthesis was designed as follows: two peptide fragments, each containing two copies of the target sequence, were synthesised by microwave-assisted *Fmoc* chemistry, as described above. Each fragment was differentiated from the other due to one of them having a cysteine residue coupled at its *C*-terminus and a cysteine residue coupled at the *N*-terminus of the second fragment. After synthesis and cleavage for releasing both peptide fragments from the resin, each peptide fragment was independently purified and characterised by RP-HPLC and identified by MALDI-TOF mass spectrometry and analysed by circular dichroism (CD) [12].

SDDC 38987 was selected for computer analysis for obtaining molecular models best representing this synthetic compound. Characterisation experiment results can be observed in Supplementary data.

2.5.3. SDDC and CLC physicochemical characteristics

Standard non-controlled Cys oxidation-produced polymers were created in all cases, having overall yield ranging from 1.7% to 3.1%, depending on the polymerised target sequence. CLCs were obtained in overall yields ranging from 1.2% to 24.3%; conventional asymmetric double dimer constructs (ADDC) overall yields were 2.1–5.6% and SDDC were obtained having 1.5–5.8% yield.

SDDC final yield was 8% for SDDC **38986** and 2% for SDDC **38990** (Fig. S1 Supplementary material and Table 1); such values came within the expected range for this type of molecule. The characteristics for symmetrical double dimers from HABPs 34273 can be observed in (Fig. S1, Supplementary material and Table 1). SDDC **38991** experimental molecular mass matched the expected mass.

Despite the differences observed in both molecules' synthesis, overall final yield was 3.5% for SDDC **38987** and 3.1% for SDDC **38991**; synthesis difficulties related to steric hindrance thus had no effect on final yield regarding their CLCs.

Greater difficulty regarding synthesis was detected in the synthesis profiles for HABP 34270's four linear fragments, as well as those for the conventional dimer analogues. The aforementioned linear fragments had no marked differences regarding synthesis steps judged to be satisfactory by reaction progress.

There were also similar synthesis profiles for the second copy in the sequence as there was less synthesis hindrance for fragments **39098** and **39099**, where an aminohexanoic acid molecule had been coupled as spacer in both cases.

The chromatographic patterns of the two pure linear fragments (both having cathepsin motifs as spacer) displayed a wide base at long elution times (characteristic of hydrophobic species); mass spectra showed that the experimental molecular masses had the expected molecular weight in each case and overall yield was 0.3% for fragment **39051** and 1% for **39052**. Such low yields prevented derivatising being continued for fragment **39051** for producing its respective peptide-Cys (Pys) for direct condensation with fragment **39052**. This drawback led to deciding on the standard oxidation of the Cys at the *N*-terminus of the **39052** linear fragment; a controlled-polymer tetramer species was thus produced, as detected by mass spectrometry analysis. Overall yield was 1% for this controlled-polymer having four copies from the target sequence. Yield was 10% for fragment **39098** and 17% for **39099** after they had been purified; this led to derivatisation being continued and subsequent condensation in a 1.14:1 eq. ratio, thereby obtaining CLC **39104** whose mass spectrometry analysis revealed an expected molecular mass. Estimated final yield for this CLC was 0.3%.

Synthesis profiles corresponding to four fragment precursors of CLCs and the conventional ADDC for modified HABP 34273 were

Table 1
*Pf*ASP HABP 34270 and 34273 macromolecule constructs.

Peptide/ Construct	Aminoacid Sequence/ compound	Obtained product (mg)	Yield (%)	Immunogen -test- group	Mouse code
36936	CGGGLGIGTGSGTGGRTGYVPGC (Human papilloma virus-L2)	7.00	3.4	**1**	1-4
38534	CGLRESEGSTYLMDKLFKKLSEGC	5.00	3.1	**2**	5-8
38986	(LRESEGSTYLMDKLFKKLSEVLFV)$_2$**ßAla**KGC	14.00	5.8	**3**	9-12
38990	(LRESEGSTYLMDKLFKKLSEFLAS)$_2$**ßAla**KGC	3.50	1.5	**4**	13-16
39106	(LRESEGSTYLMDKLFKKLSE)$_2$KGC	6.40	2.1	**5**	17-20
39052	**C**FLASLRESEGSTYLMDKLFKKLSEVLFVLRESEGSTYLMDKLFKKLSE **C**FLASLRESEGSTYLMDKLFKKLSEVLFVLRESEGSTYLMDKLFKKLSE	1.50	0.4	**6**	21-24
39104	LRESEGSTYLMDKLFKKLSEAhxLRESEGSTYLMDKLFKKLSE**C**- **-C**AhxLRESEGSTYLMDKLFKKLSEAhxLRESEGSTYLMDKLFKKLSE	3.40	3.4	**7**	26-27
38538	CGNKYMYMNDVQSILNNHHLENGC	7.10	1.7	**8**	29-32
38987	(NKYMYMNDVQSILNNHHLENVLFV)$_2$**ßAla**KGC	6.40	2.8	**9**	33-36
38991	(NKYMYMNDVQSILNNHHLENVLFV)$_2$**ßAla**KGC	5.70	2.3	**10**	37-40
39107	(NKYMYMNDVQSILNNHHLEN)$_2$KGC	17.60	5.6	**11**	41-44
39103	NKYMYMNDVQSILNNHHLENFLASNKYMYMNDVQSILNNHHLENVLFV**C**- **-C**FLASNKYMYMNDVQSILNNHHLENVLFVNKYMYMNDVQSILNNHHLEN	2.40	24.3	**12**	45, 47, 49, 50
39105	NKYMYMNDVQSILNNHHLENAhxNKYMYMNDVQSILNNHHLEN**C**- **-C**AhxNKYMYMNDVQSILNNHHLENAhxNKYMYMNDVQSILNNHHLEN	2.00	1.2	**13**	51-54
Placebo	Saline solution	ND	ND	**14**	46, 48, 55, 56

also processed. As observed when constructing 34270 linear fragments, minor synthesis difficulties were encountered when constructing the second copy of the target sequence for linear fragments **39100** and **39101**; aminohexanoic acid coupling was thus used. Overall yield for this group of ADDCs was 2.1% for construct 39106 and 6.6% for 39107.

2.6. Plasmodium berghei and Plasmodium yoelii infection of BALB/c mice vaccinated with modified polymerised and macromolecule construct forms of PfASP HABPs

Cryopreserved *P. yoelii* 17XL and *P. berghei* ANKA rodent malarial strains stored in Krebs solution (0.85% NaCl, 5% glucose and 4.2% (p/v) sorbitol) were thawed, heated at 37 °C and washed with a non-supplemented RPMI medium to produce *in vivo* malarial infection in BALB/c mice. Experimental challenge involved both *in vivo*-obtained strains (40–50% parasitaemia) being independently centrifuged at 1500 rpm for 5 min; the pellet containing about 1×10^7 infected red blood cells (iRBC) was suspended in 1 mL RPMI and immediately used for either intravenously (iv) or intra-peritoneal (ip) inoculation. Each animal was injected with 5×10^4 iRBC. Parasitaemia in all infected animals was monitored by Wright and acridine-orange staining of blood-smears; this showed that mice became parasitised by the second to sixth day after infection and that parasitaemia levels increased faster until animals died 12–15 days after having been infected. Parasitaemia follow-up was performed according to experimental requirements. Animal care was in accordance with FIDIC's institutional guidelines. Animals subjected to invasive procedures were treated under anaesthetic, analgesic and tranquilising conditions and intra-muscularly (im) injected with a combination of 150 mg/kg ketamine/ 10 mg/kg xylazine.

3. Results and discussion

3.1. Bioinformatics and PfASP B-epitopes

*Pf*ASP (PFD0295) sequence analysis using Antheprot and BepiPred servers led to selecting 4 sequences as being potential B-epitopes. These *Pf*ASP sequences were coded 34276, 34278, 34280 and 34283 and used for rabbit inoculation, as described in Section 2. *Pf*ASP genetic polymorphism is shown in Fig. 1A and B.

Polyclonal antibodies were stimulated in rabbits immunised with mixtures of monomer forms of two predicted B-epitopes (rabbits 99 and 72 inoculated with peptide mixture 34276/34278 and rabbits 100 and 101 inoculated with 34280/34283); formulations were supplemented with FIS, a non-specific T-epitope [7], and stimulated antibodies were used for *P. falciparum* detection in immunochemical assays [13]. Induced antibodies specifically recognised a band located about 52 kDa whose relative mobility could have corresponded to the previously reported 50 kDa C-terminal *Pf*ASP processed fragment (Fig. 1C) [14]. Another two bands were also detected (one at 78 kDa and a faster one at 49 kDa). IFA experiments led to such induced antibodies recognising *P. falciparum* asexual stages, thereby contrasting with the non-reactivity displayed by the pre-immune sera sample shown in Fig. 1D.

3.2. PfASP high activity binding peptide (HABP) determination

Radiolabelling experiments led to detecting another four *Pf*ASP peptide sequences characterised by their high specific binging to *Plasmodium* target cells (erythrocytes). These novel molecules were classified as HABPs, as previously discussed, and coded 34259, 34270, 34273 and 34290; they were located in *Pf*ASP semi-conserved and conserved regions, the latter belonging to the sushi

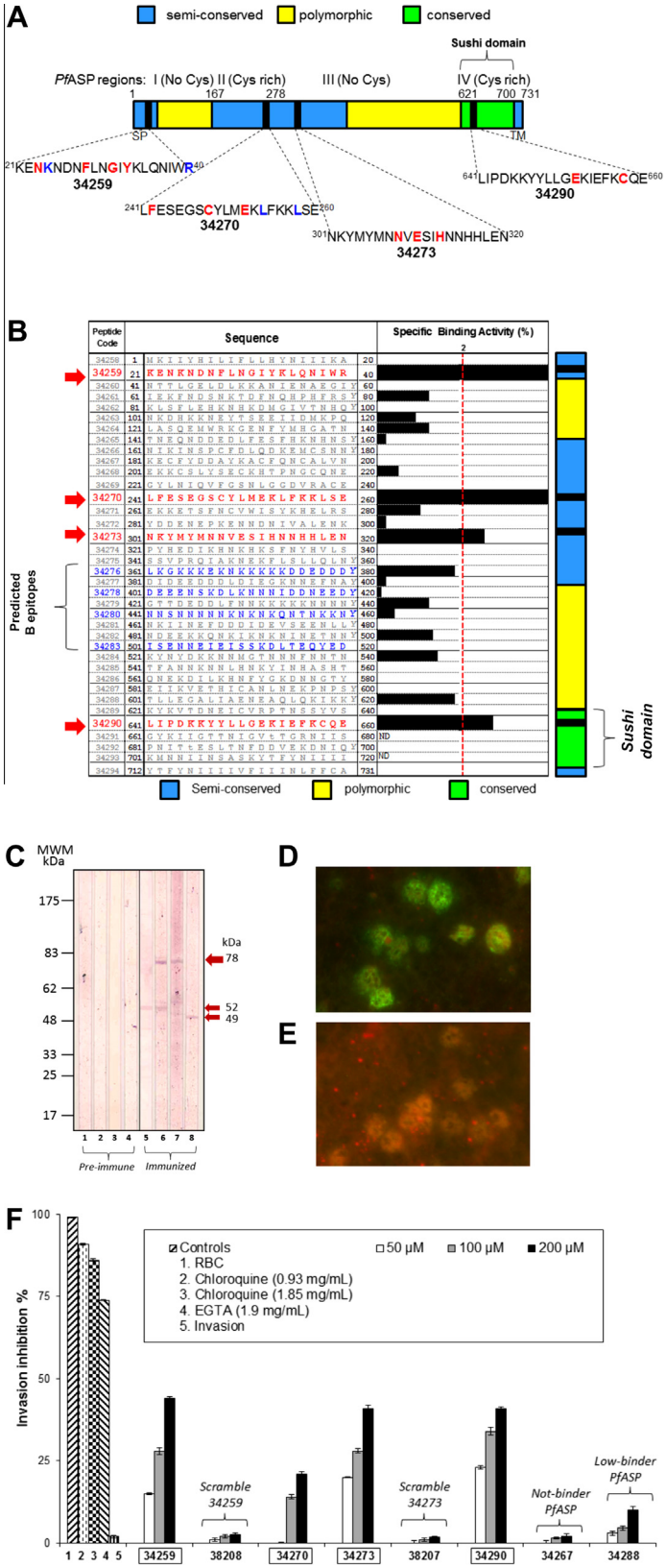

Fig. 1. *Plasmodium falciparum* ASP antigenic potential and red blood cell binding properties. (A) Genetic organisation and functional sequence detection. (B) Determining high activity binding peptides in *Pf*ASP. (C) Western blot analysis of *Plasmodium falciparum* merozoite protein lysate rabbit antibodies. (D) IFA experiments regarding polyclonal antibody reactivity revealed antigens expressed in mature schizonts. (E) Pre-immune serum non-reactivity. (F) *Pf*ASP-HABPs capacity for inhibiting *Plasmodium falciparum* FCB-2 invasion of human RBC. The *Pf*ASP sequence was analysed with 20-mer long non-overlapping peptides. The Figure shows each HABP sequence in red and predicted B-epitopes in blue and their location within the protein's primary structure.

domain at the protein C-terminus (Fig. 1B). Higher than 2% specific binding was considered to be statistically significant. Fig. 1E shows that *Pf*ASP selected HABPs had functional activity by avoiding *P. falciparum* invasion of RBC in a dose-dependent manner. The *P. falciparum* FCB-2 chloroquine sensitive strain could not efficiently invade RBC when HABP 34259, 34273 and 34290 were present in culture medium. HABP 34270 inhibited *Plasmodium* invasion to a lesser degree. Scrambled peptides, based on the native sequences of some *Pf*ASP-HABPs, did not have functional or inhibiting activity, nor did the non-relevant VPH-L2 sequence and *Pf*ASP sequences determined as being non-binders or low-binders. None of the above predicted B-epitopes matched the new *Pf*ASP HABP family. However predicted B-epitope 34276 showed a mild capacity for RBC binding. Most *Pf*ASP-HABPs were neither haemolytic nor toxic for eukaryotic cells (Fig. S2 in Supplementary material).

3.3. Determining PfASP HABP critical binding residues

HABP 34259 had two critical binding residues, i.e. ^{1}Arg and ^{16}Lys. These residues were identified by taking native radiolabelled-HABP binding as being 100% and competition binding assays with increasing Gly-analogue concentrations led to this value becoming reduced to less than 50%. Likewise, two Leu residues in positions 3 and 7 were determined to be critical, non-polar, residues for HABP 34270 binding to RBC.

No critical residues were detected for HABP 34273 and 34290 binding to RBCs at any of the concentrations tested here. The results suggested that all residues were important for these two HABPs' binding, thereby implicating possible secondary structure-mediated mechanisms.

3.4. Synthesis of symmetric double dimer and condensed linear constructs

One of our institute's objectives has been to find a strategy for obtaining a multicopy antigen-presenting molecule which could be 100% characterisable as a single molecular species [15]. However such strategy could not be extrapolated to any antigen peptide sequence, probably due to many chemical restrictions occurring during synthesis, i.e. conformational or differential reactivity between chemical functions, especially those involving amino groups located at both α and ε positions on a Lys residue (this being the basis for conventional dendrimer peptide constructs). The present research was thus aimed at minimising the difference in distance and reactivity between both lysine amino groups regarding α-carbon and determining their possible effect on the efficiency of synthesising such new constructs.

The synthesis of a symmetrical macromolecular construct was thus designed, involving condensing a β-alanine residue to the lysine alpha amino group; the distance between lysine α and ε amino functions was comparable regarding α-carbon, thus making reactivity equivalent for these two new amino functions (synthesis strategy is shown in Fig. S3, Supplementary material). This new type of tetra-branched molecule was called a symmetric double dimer construct (SDDC).

The new β-Ala-Lys bi-functional core was subsequently assessed for obtaining SDDC by anchoring the *Pf*ASP HABP selected sequences to its four branches; eight SDDC were thus designed and synthesised, two for each modified analogue (Table 1).

SDDC design arose from the hypothesis of introducing specific cathepsin oligo-peptide substrates as spacers between each core's branch and the *Pf*ASP analogue sequence to guide or modulate the

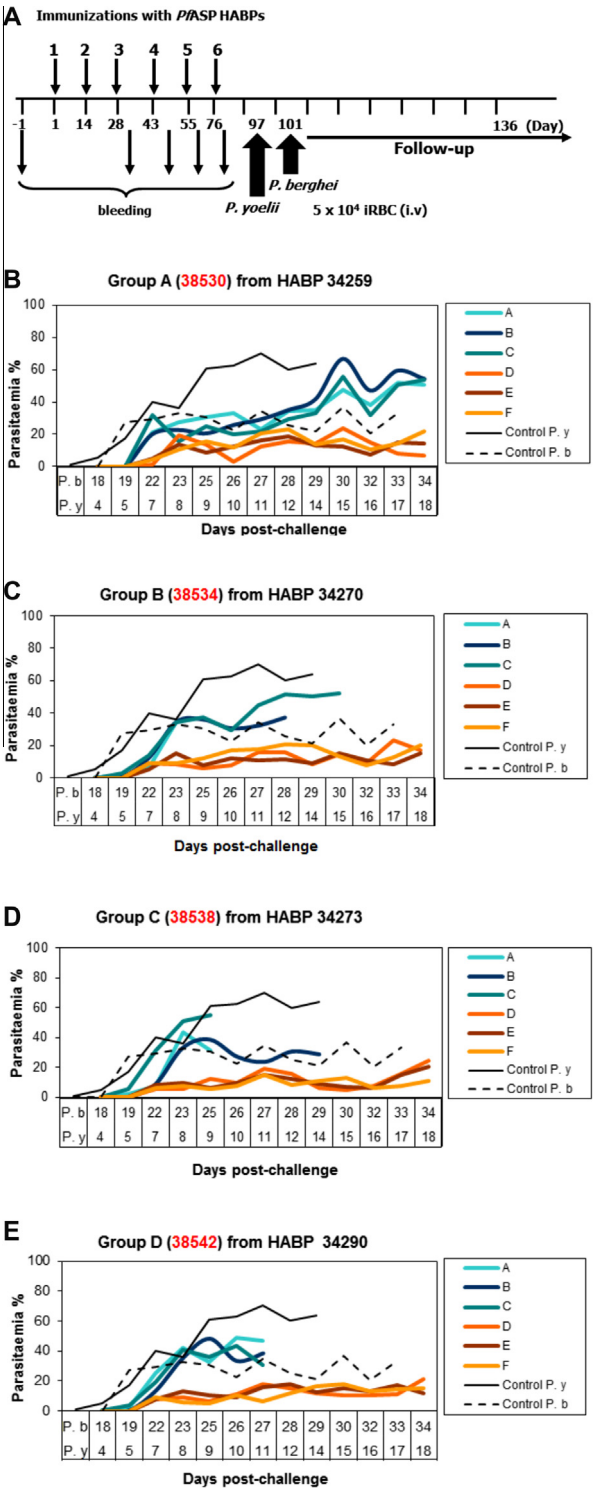

Fig. 2. *Pf*ASP-HABPs *in vivo* functional activity. (A) Immunisation schedule for BALB/c mice vaccination with *Pf*ASP-HABP analogues and controlled challenge with two malarial rodent strains. (B) Group A injected with modified HABP 34259 derived from the **38530** sequence. (C) Group B inoculated with 34270-derived modified HABP **38534**. (D) Group C immunised with 34273-derived **38538**. (E) Group D injected with 34290-derived **38542**. Blue infection profiles represent mice challenged with *P. yoelii*, red-orange infection profiles those challenged with *P. berghei* and black profiles represent infected control group challenged with *P. yoelii* (solid line) and *P. berghei* (dotted line).

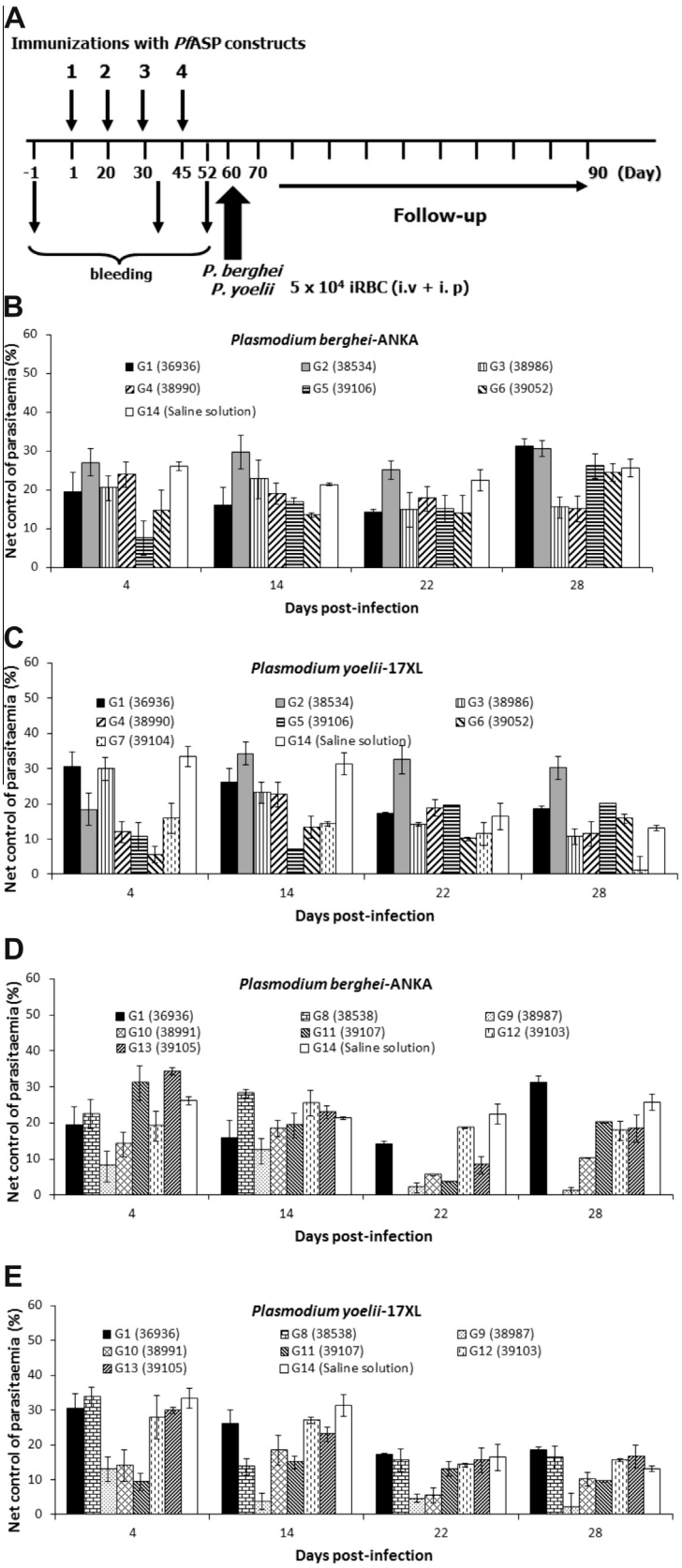

Fig. 3. *Pf*ASP-derived tetramer constructs' protection-inducing capacity. (A) Immunisation schedule for BALB/c mice vaccination with *Pf*ASP-tetramer constructs and experimental challenge with two rodent malarial strains. (B) Net control of parasitaemia in mice vaccinated with **38534** constructs and challenged with *P. berghei*. (C) Net control of parasitaemia of mice vaccinated with **38534** constructs and challenged with *P. yoelii*. (D) Net control of parasitaemia of mice vaccinated with **38538** constructs and challenged with *P. berghei*. (E) Net control of parasitaemia of mice vaccinated with **38538** constructs and challenged with *P. yoelii*.

macromolecule complex during *in vivo* processing by antigen presenting cells (APC). Cathepsin Val-Leu-Phe-Val and Phe-Leu-Ala-Ser substrates were thus selected [16,17].

Design also took analogue sequence modification into account, considering predicted HLA-DR allele reading frames, especially HLA-DR associated with ethnic characteristics [4]. This approach was adopted, given that not all derived HABPs had any critical target cell binding residues or binding motifs. Fig. 1A and B gives the chosen HABP sequences.

Each HABP analogue peptide containing the Gly–Cys pair at their amino and carboxyl-termini was also synthesised. Likewise, original HABP sequences were also synthesised as polymer forms to be further evaluated in *in vivo* studies, along with their modified analogues.

Three modified analogues were designed from HABP 34259; mutations were made in ^{8}Tyr, ^{10}Gly, ^{13}Phe and ^{18}Asn residues. One analogue was derived from HABP 34270, having changes in ^{9}Glu and ^{19}Phe, three from HABP 34273 having changes in ^{8}His and ^{11}Glu and ^{13}Asn and two analogues from HABP 34290 mutated in ^{9}Glu. HABPs 34270 and 34290 contained a Cys residue in their original sequence; this amino acid was replaced with a Thr residue to prevent unwanted species due to Cys oxidation when finishing

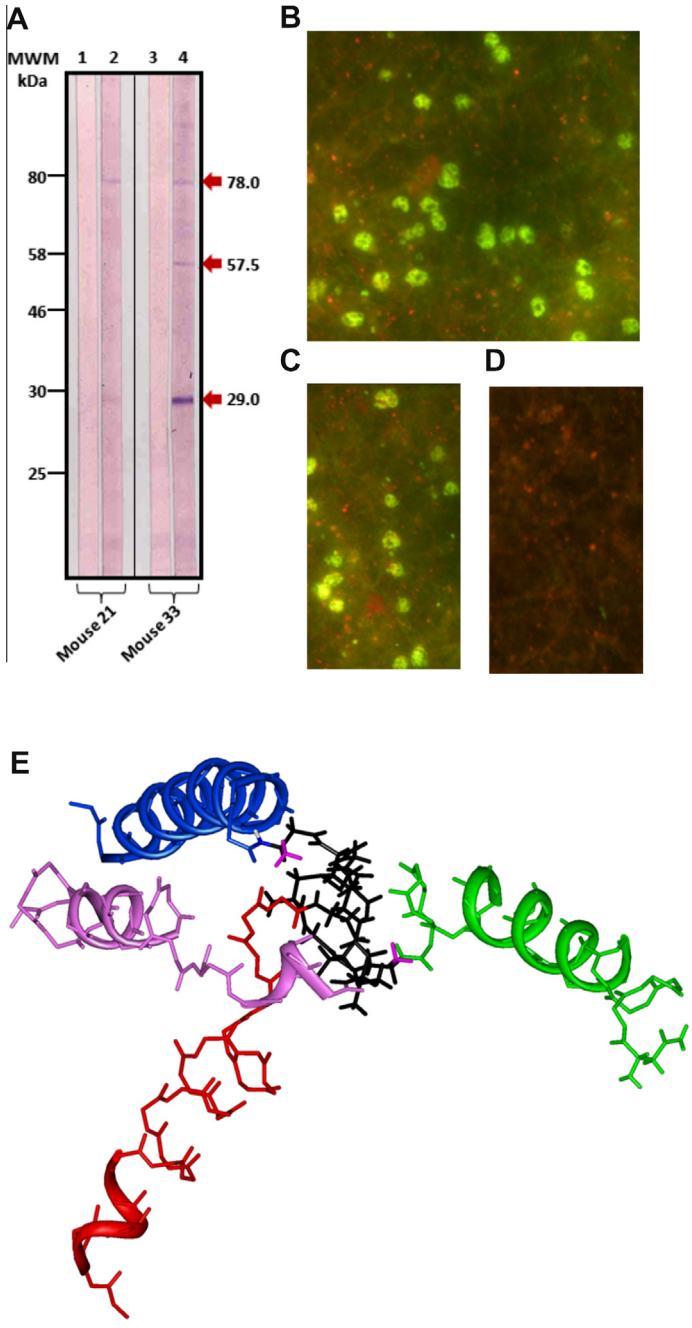

Fig. 4. Protected animals' antibody reactivity to *P. falciparum* proteins. (A) Western blot analysis of *P. falciparum* merozoite protein lysate mouse antibodies. Lanes 1 and 3 show pre-immune sera reactivity; lanes 2 and 4 display protected mouse antibody reactivity to *Pf*ASP. (B) IFA experiments regarding protected mouse 21 antibody reactivity. (C) IFA reactivity of mouse 33 to *P. falciparum* mature schizonts. (D) Pre-immune serum non-reactivity to antigens expressed in mature schizonts. (E) Molecular model representing SDDC **38987**. *Pf*ASP peptide-branches: α-helixes in red, green, lilac and blue. Symmetrical core is shown in black.

synthesis. Each peptide was designed to contain a Cys residue at both *C*- and *N*-terminal positions of each designed and synthesised analogue.

Fig. S4 (Supplementary material) shows that a three-step rational strategy for obtaining condensed linear constructs (CLC) was followed, based on orthogonal condensation of two *Pf*ASP-sequence building blocks.

3.5. Secondary structure profile of tetramer constructs

Each synthesised macromolecule construct's secondary structure elements were evaluated by CD experiments; analysis involved two systems: molecule dissolved in water and 30% TFE in water (Fig. S1 in Supplementary material). The spectra for HABP 34270 construct analogues revealed an α-helical trend in both water and 30% TFE, except for construct **39052** (the tetramer polymer); these results suggested that this particular sequence's structure profiles were preserved, regardless of synthesis construction.

HABP 34273 analogue constructs had α-helical structure elements in spectra recorded in 30% TFE in which defined trends were observed, except for construct **38991** (symmetrical construct SDDC) involving a structure shift. However, this particular sequence's structural trend was conserved.

3.6. Protective efficacy of PfASP macromolecular constructs

*Pf*ASP harbours HABPs 34259, 34270, 34273 and 34290**,** all having poorly haemolytic activity (less than 15%) and less than 50% cytotoxic activity at 0.50 mg/mL; their derived tetramer constructs have also proved to have non-haemolytic activity (less than 1.0%) and less than 30% cytotoxic activity at the highest concentration (0.50 mg/mL), as shown in Fig. S1 (Supplementary material).

Immunisation and rodent malaria challenge experiments with *Pf*ASP modified HABPs were subsequently conducted in mice. Animals were distributed into groups and were immunised with conventional non-controlled polymer forms of both original HABPs and their modified versions. Modified HABP **38530** (^{21}PfASP^{40}) from HABP 34259, 34270-derived modified HABP **38534** (^{241}PfASP^{280}), 34273-derived **38538** (^{301}PfASP^{320}) and 34290-derived **38542** (^{641}PfASP^{660}) were used as immunogens, according to the schedule shown in Fig. 2A. Groups of mice were split up before being challenged with *P. yoelii* and *P. berghei*. Kinetic infection was faster and greater in groups of animals injected with saline solution (placebo) and which did not survive the experiment. In all cases animals challenged with *P. yoelii* had higher parasitaemia patterns (associated with its virulence) than those challenged with *P. berghei* (as seen in Fig. 2). Animals vaccinated with HABPs were able to control parasitaemia and resolved infection in some cases, thereby showing antigenic and immunological profiles required by candidates for macromolecule design.

A macromolecule version of each modified HABP was designed and synthesised amongst SDDCs and CLFs and used in a new set of vaccination experiments (Table 1). Groups of six mice were randomly distributed and vaccinated as shown in Fig. 3A and Table 1; they were then split up and challenged simultaneously iv and ip with 5×10^4 *P. yoelii* and *P. berghei* iRBC, respectively. Parasitaemia was follow-up during 30 days post-challenge. Fig. 3 shows that animals vaccinated with non-relevant HPV-L2-derived 36936 (group 1) as well as a non-controlled polymer version for modified HABPs **38534** (group 2) and **38538** (group 8) did not control malarial infection in both cases and had high parasitaemia levels (like animals in placebo group 14).

Remarkably, modified HABP **38534**-derived double dimer **39106** (group 5), linear condensed controlled polymer **39052** (group 6) and SDDC **38986** (group 3) and modified HABP **38538**-derived SDDC **38987** (group 9), SDDC **38991** (group 10) and double dimer **39107** (group 11) all had better control of parasitaemia and disease resolution in experimental conditions. Fig. 4A shows that sera antibodies from protected mouse 21 vaccinated with CLC **39052** and mouse 33 vaccinated with SDDC **38987** specifically recognised *P. falciparum* lysate bands at 78.0, 57.5 and 29.0 kDa, thereby revealing a specific immune response to the pathogen. Both mice antibody samples strongly recognised *P. falciparum* mature schizonts in IFA experiments (Fig. 4B–D).

3.7. Tetramer molecular structure model

The 3D structure model representing tetramer SDDC **38987** was molecularly modelled using Insight II Discover software (Secondary Render Molecule: Kabsch_Sander). QMean Z-score was −5.668, representing an acceptable/special-likely model [18]. Some features of the proposed molecular model for this SDDC's symmetrical core can be seen in Fig. 4E.

Cys-polymers were obtained during conventional non-controlled oxidation, based on their binding motifs and predicted HLA-DR reading frames, and immunologically tested. These molecules were neither toxic nor haemolytic; such desirable characteristics make them safe and harmless. SDDC and CLC chemically-defined polymer forms from *Pf*ASP modified HABPs 34270 **(38534)** and 34273 **(38538)** were designed, synthesised and characterised as SDDC and CLC macromolecule-antigen presenting systems, based on previous knowledge [19,20].

This work has demonstrated that SDDC and CLC synthesis for obtaining tetramer-defined molecules as a unique molecular species is feasible and represents excellent large platforms for the formulation of antimalarial vaccine candidates and should be explored at more complex levels in vaccinology studies.

Acknowledgments

The authors are indebted to co-workers and scientists from Fundación Instituto de Inmunología de Colombia (FIDIC) for experimental support and the Colombian Science, Technology and Innovation Department (Colciencias) **(Grant 212456934488)**. The *Plasmodium yoelii*-17XL strain was a kind gift from Prof. Lilian Spencer-Valero from Universidad Simón Bolívar's Cell Biology Department (Caracas, Venezuela) and the *Plasmodium berghei*-ANKA strain was a kind gift from Prof. Silvia Blair from the Universidad de Antioquia's Medicine Faculty's malaria laboratory (Medellin, Colombia). Special thanks are given to Jason Garry for help provided in translating the manuscript.

Appendix A. Supplementary data

Supplementary data associated with this article can be found, in the online version, at http://dx.doi.org/10.1016/j.bbrc.2014.06.143.

References

[1] World Health Organization, World Malaria Report 2012, Global Malaria Programme, 20, avenue Appia, CH-1211 Geneva 27, URL Web: <http://www.who.int/malaria>, Switzerland, 2012 (accessed on October 8th, 2013).
[2] R.G. Ridley, Malaria: to kill a parasite, Nature 424 (2003) 887–889.
[3] T.L. Richie, A. Saul, Progress and challenges for malaria vaccines, Nature 415 (2002) 694–701.
[4] M.E. Patarroyo, M.A. Patarroyo, Emerging rules for subunit-based, multiantigenic, multistage chemically synthesized vaccines, Acc. Chem. Res. 41 (2008) 377–386.
[5] A.D. Attie, R.T. Raines, Analysis of receptor–ligand interactions, J. Chem. Educ. 72 (1995) 119–123.
[6] C. Geourjon, G. Deleage, B. Roux, Antheprot: an interactive graphics software for analyzing protein structures from sequences, J. Mol. Graphics 9 (1991) 188–190.
[7] J.E. Larsen, O. Lund, M. Nielsen, Improved method for predicting linear B-cell epitopes, Immunome Res. 2 (2006) 2.

[8] A. Puentes, J. Garcia, M. Ocampo, L. Rodriguez, R. Vera, H. Curtidor, R. López, J. Suarez, J. Valbuena, M. Vanegas, F. Guzman, D. Tovar, M.E. Patarroyo, *P. falciparum*: merozoite surface protein-8 peptides bind specifically to human erythrocytes, Peptides 24 (2003) 1015–1023.
[9] L.E. Rodríguez, H. Curtidor, M. Urquiza, G. Cifuentes, C. Reyes, M.E. Patarroyo, Inti-mate molecular interactions of *P. falciparum* merozoite proteins involved in invasion of red blood cells and their implications for vaccine design, Chem. Rev. 108 (2008) 3656–3705.
[10] C. Lambros, J.P. Vanderberg, Synchronization of *Plasmodium falciparum* erythrocytic stages in culture, J. Parasitol. 65 (1979) 418–420.
[11] L. Fischer, C. Didierjean, F. Jolibois, V. Semetey, J.M. Lozano, J.-P. Briand, M. Marraud, R. Poteauc, G. Guichard, Propensity for local folding induced by the urea fragment in short-chain oligomers, Org. Biomol. Chem. 6 (2008) 2596–2610.
[12] D. Roccatano, G. Colombo, M. Fioroni, A.E. Mark, Mechanism by which 2,2,2-trifluoroethanol/water mixtures stabilize secondary-structure formation in peptides: a molecular dynamics study, Proc. Natl. Acad. Sci. U.S.A. 99 (2002) 12179–12184.
[13] I. Prieto, S. Hervás-Stubbs, M. García-Granero, C. Berasain, J.I. Riezu-Boj, J.J. Lasarte, P. Sarobe, J. Prieto, F. Borrás-Cuesta, Simple strategy to induce antibodies of distinct specificity: application to the mapping of gp 120 and inhibition of HIV-1 infectivity, Eur. J. Immunol. 25 (1995) 877–883.
[14] A.H. O'Keeffe, J.L. Green, M. Grainger, A.A. Holder, A novel Sushi domain-containing protein of *Plasmodium falciparum*, Mol. Biochem. Parasitol. 140 (2005) 61–68.
[15] Z.Y. Rivera, G. Granados, M. Pinto, D. Varón, C. Carvajal, F. Chaves, J. Calvo, R. Rodríguez, F. Guzmán, M.E. Patarroyo, Double dimer peptide constructs are immunogenic and protective against *Plasmodium falciparum* in the experimental Aotus monkey model, J. Pept. Res. 59 (2002) 62–70.
[16] C.C. Clement, L. Santambrogio, The lymph self-antigen repertoire, Front. Immunol. 4 (2013) 424.
[17] A. Vaithilingam, N.Y. Lai, E. Duong, J. Boucau, Y. Xu, M. Shimada, M. Gandhi, S. Le Gall, A simple methodology to assess endolysosomal protease activity involved in antigen processing in human primary cells, BMC Cell Biol. 14 (2013) 35.
[18] P. Benkert, M. Biasini, T. Schwede, Toward the estimation of the absolute quality of individual protein structure models, Bioinformatics 27 (2011) 343–350.
[19] J.M. Lozano, F. Espejo, R. Vera, L.E. Vargas, J.E. Rosas, L.P. Lesmes, E. Torres, J. Cortés, Y. Silva, M.E. Patarroyo, Protection against malaria induced by chirally-modified *Plasmodium falciparum's* MSP1-42 pseudopeptides, Biochem. Biophys. Res. Commun. 329 (2005) 1053–1066.
[20] J.J. Pérez-Cordero, J.M. Lozano, J. Cortés, G. Delgado, Leishmanicidal activity of synthetic antimicrobial peptides in an in vitro infection model with human dendritic cells, Peptides 32 (2011) 683–690.